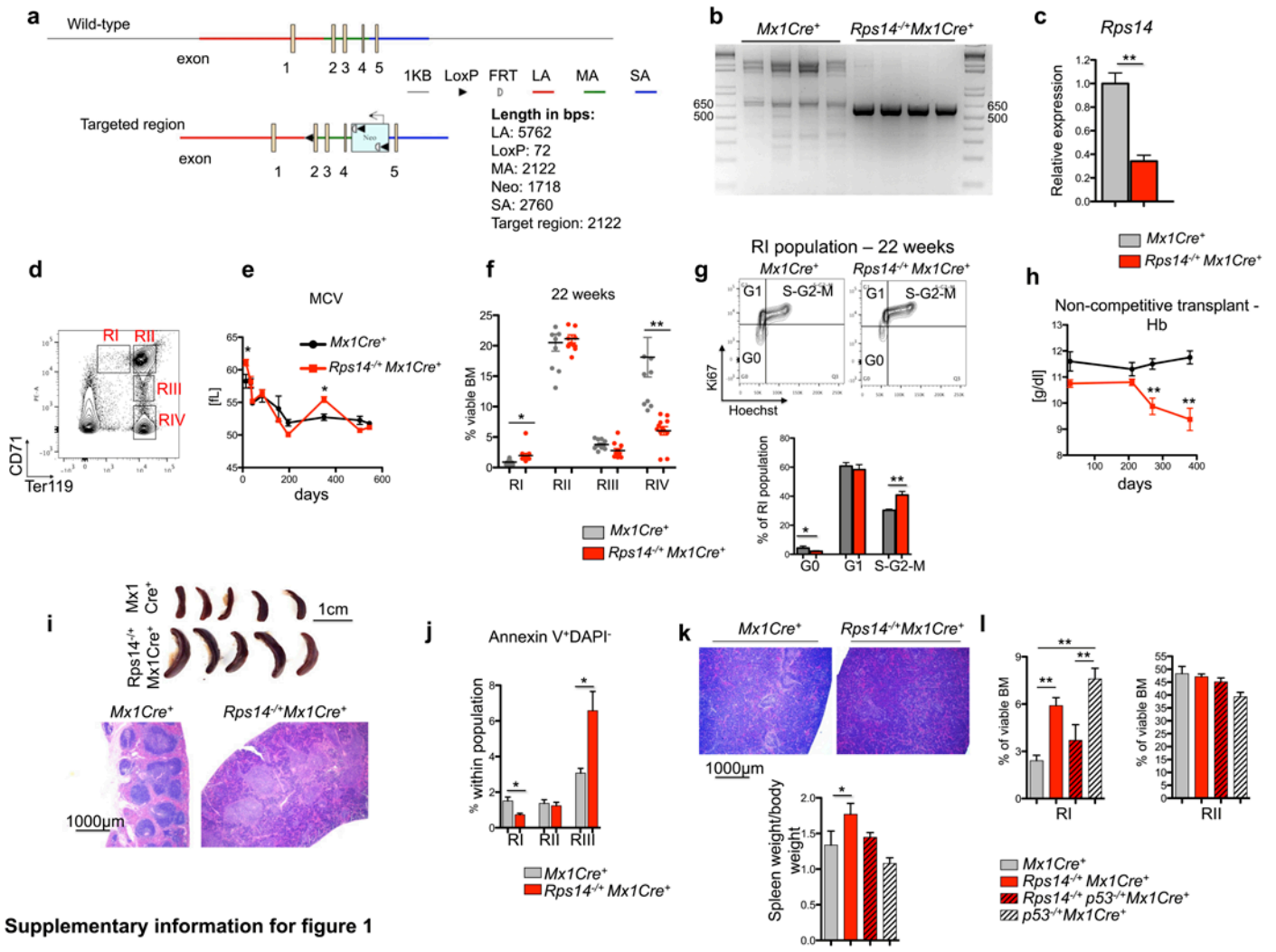

Supplementary information for figure 1

Supplementary figure 1: **Targeting construct and consequences of *Rps14* haploinsufficiency on the erythroid phenotype.** (a) Schematic of the targeting construct. The *Rps14* target region is 2.12 Kb and includes exon 2-4. The region was designed such that the 5' homology arm extends about 5.76 Kb 5' to the single LoxP. The 3' homology arm ends 3' to the loxP/FRT flanked Neo cassette and is 2.76 Kb long. The loxP/FRT flanked Neo cassette was inserted 255 bp downstream of exon 4. The single loxP site was inserted 379 bp upstream of exon 2. The total size of the targeting construct (including vector backbone and Neo cassette) was 14.74 Kb. (b) Excision PCR confirming the removal of the targeted region 10 days after poly(I:C) injection in Rps14$^{-/+}$Mx1Cre^{+} but not *Mx1Cre*$^{+}$ control cells. (c) Quantification of *Rps14* transcript levels by quantitative real-time PCR in lineage-negative bone marrow cells 10 days after poly(I:C) injection. Data are normalized to expression in *Mx1Cre*$^{+}$ control cells (n=8; mean±SD, **p<0.001). (d) Representative flow blot for the gating strategies of the RI-RIV erythroid progenitor populations by CD71 and Ter119 staining. Region I (CD71^{high}Ter119^{intermediate}) reflects proerythroblasts, region II are basophilic erythroblasts (CD71^{high}Ter119^{+}), region III represents late basophilic and chromatophilic erythroblasts (CD71^{intermediate}Ter119^{+}) and region IV orthochromatophilic erythroblasts (CD71^{-}Ter119^{+}) (according to Socolovsky et al. 2001). (e) Mean corpuscular volume (MCV) of red blood cells in the peripheral blood from *Rps14*$^{-/+}$*Mx1Cre*$^{+}$ mice in comparison to *Mx1Cre*$^{+}$ wild-type controls. (mean±SD, n=10; *p<0.05). (f) Quantification of the frequencies of the RI-RIV population in *Mx1Cre*$^{+}$ and *Rps14*$^{-/+}$*Mx1Cre*$^{+}$ mice 22 weeks after poly(I:C); (mean±SD, n=10 for *Mx1Cre*$^{+}$; 12 for *Rps14*$^{-/+}$*Mx1Cre*$^{+}$; *p<0.05; **p<0.001). (g) Cell cycle analysis using combined Ki67 and Hoechst staining within cells stained with CD71 and Ter119. Representative flow plots and quantification of the frequencies of RI cells within the G0, G1 and S-G2-M phase in *Mx1Cre*$^{+}$ and *Rps14*$^{-/+}$*Mx1Cre*$^{+}$ mice 22 weeks after poly(I:C). (mean±SD, n=10 for *Mx1Cre*$^{+}$; 12 for

Rps14$^{-/+}$*Mx1Cre*$^{+}$; *p<0.05; **p<0.001). (h) Hemoglobin kinetics in wild-type recipient mice (CD45.1) that were transplanted with *Mx1Cre*$^{+}$ and *Rps14*$^{-/+}$*Mx1Cre*$^{+}$ whole bone marrow cells 4 weeks after poly(I:C). (n=5; mean±SD, **p<0.001). (i) Representative macroscopical and histopathological images of spleens in *Mx1Cre*$^{+}$ and *Rps14*$^{-/+}$*Mx1Cre*$^{+}$ mice 18 months after poly(I:C); (mean±SD, n=5; **p<0.001). HE-staining, 4x magnification. (j) Annexin-positive/DAPI-negative, apoptotic cells within the RI-RIII population at day 9 after Phenylhydrazine treatment in *Rps14*$^{-/+}$*Mx1Cre*$^{+}$ (n=5) and *Mx1Cre*$^{+}$ control mice (n=5), (*p<0.05). (k) Representative spleen histopathology in *Rps14*$^{-/+}$*Mx1Cre*$^{+}$, *p53*$^{-/+}$*Mx1Cre*$^{+}$, *Rps14*$^{-/+}$*p53*$^{-/+}$*Mx1Cre*$^{+}$ and *Mx1Cre*$^{+}$ control mice. Relative spleen to body weight [%] of *Mx1Cre*$^{+}$ and *Rps14*$^{-/+}$*Mx1Cre*$^{+}$ mice 9 days after the first treatment with 25mg/kg Phenylhydrazine in *Rps14*$^{-/+}$*Mx1Cre*$^{+}$ (n=14), *p53*$^{-/+}$*Mx1Cre*$^{+}$ (n=5), *Rps14*$^{-/+}$*p53*$^{-/+}$*Mx1Cre*$^{+}$ (n=5) and *Mx1Cre*$^{+}$ control mice (n=8) (mean±SD; *p<0.05). (l) Frequency of RI and RII erythroid progenitor populations among viable bone marrow cells in *Rps14*$^{-/+}$*Mx1Cre*$^{+}$ (n=5), *p53*$^{-/+}$*Mx1Cre*$^{+}$ (n=5), *Rps14*$^{-/+}$*p53*$^{-/+}$*Mx1Cre*$^{+}$ (n=5) and *Mx1Cre*$^{+}$ control mice (n=8) characterized by differential CD71 and Ter119 expression (mean±SD; **p<0.001).

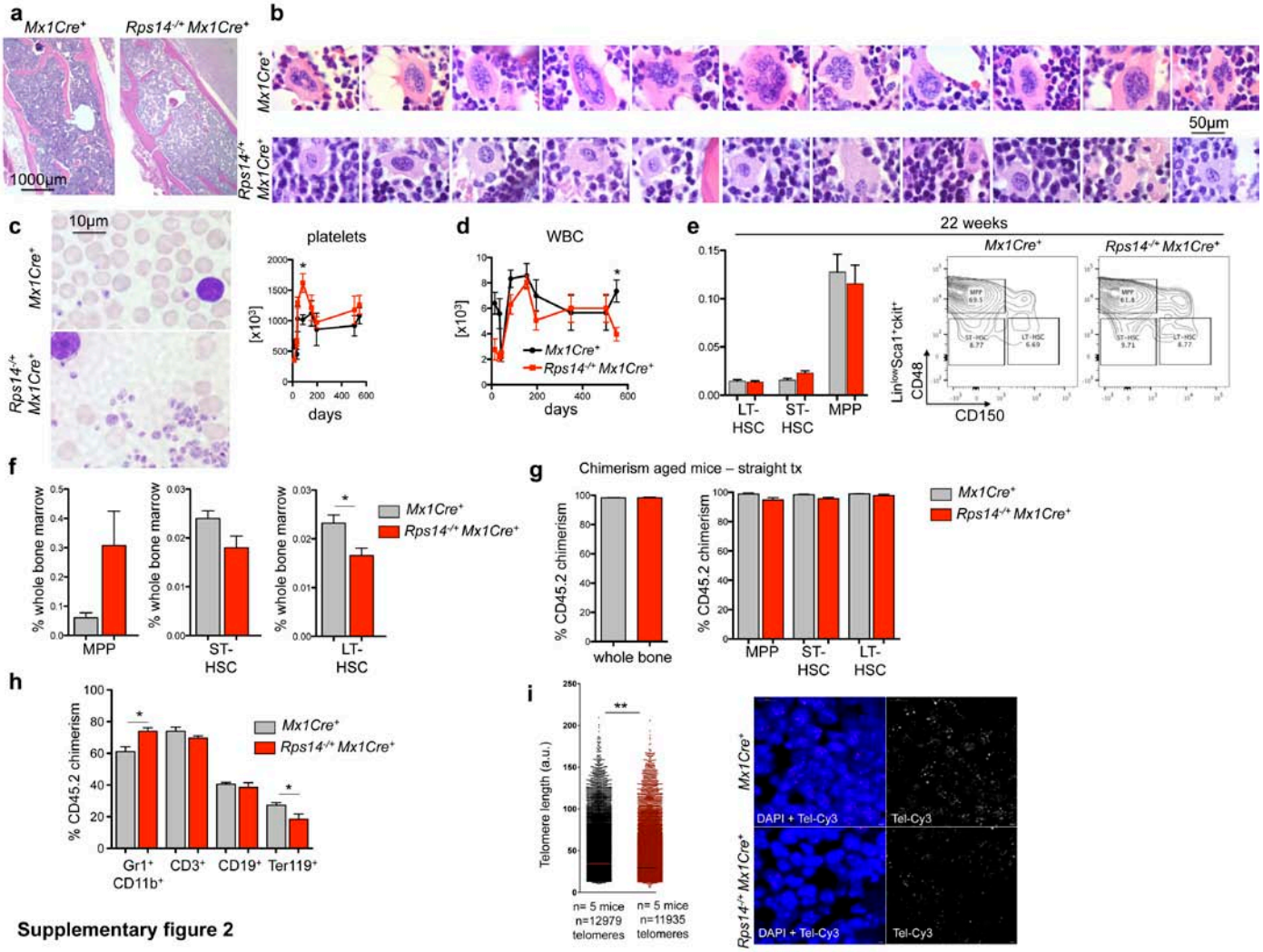

Supplementary figure 2: Hematological phenotype of *Rps14* haploinsufficient mice. (a) Histopathological overview of the spinal part of the bone marrow in *Rps14*$^{-/+}$*Mx1Cre*$^{+}$ (n=5) and *Mx1Cre*$^{+}$ mice (n=4) 18 months after the first poly(I:C) injection. HE-staining. 4x magnification. (b) Representative high-power magnification pictures (100x with oil) of HE-stained bone marrows from *Rps14*$^{-/+}$*Mx1Cre*$^{+}$ (n=5)

and *Mx1Cre*$^{+}$ mice (n=4) 18 months after the first poly(I:C) injection. (c) Representative peripheral blood smear, May-Gruenwald-Giemsa staining and platelet counts in the peripheral blood from *Rps14*$^{-/+}$*Mx1Cre*$^{+}$ mice in comparison to *Mx1Cre*$^{+}$ wild-type controls. (mean±SD, n=10; *p<0.05). (d) White blood cell (WBC) count in the peripheral blood from *Rps14*$^{-/+}$*Mx1Cre*$^{+}$ mice in comparison to *Mx1Cre*$^{+}$ wild-type controls. (mean±SD, n=10; *p<0.05). (e) Representative flow plots and frequency of MPPs (lineage^{low}ckit^{+}Sca1^{+}CD48^{+}CD150^{-}), ST-HSCs (lineage^{low}ckit^{+}Sca1^{+}CD48^{-}CD150^{-}) and LT-HSCs (lineage^{low}ckit^{+}Sca1^{+}CD48^{-}CD150^{+}) in *Mx1Cre*$^{+}$ and *Rps14*$^{-/+}$*Mx1Cre*$^{+}$ mice 22 weeks after poly(I:C).
(f) Whole bone marrow cells from primary 18 months old mice were injected in 6-8 week old SJL/CD45.1 recipient mice. Frequency of MPPs (lineage^{low}ckit^{+}Sca1^{+}CD48^{+}CD150^{-}), ST-HSCs (lineage^{low}ckit^{+}Sca1^{+}CD48^{-}CD150^{-}) and LT-HSCs (lineage^{low}ckit^{+}Sca1^{+}CD48^{-}CD150^{+}) 6 weeks after transplantation in *Rps14*$^{-/+}$*Mx1Cre*$^{+}$ (n=5) and *Mx1Cre*$^{+}$ mice (n=4); (mean±SD; *p<0.05). (g) Whole bone marrow donor chimerism (CD45.2) and donor chimerism in MPPs, ST-HSCs and LT-HSCs of 18 months old whole bone marrow cells from *Rps14*$^{-/+}$*Mx1Cre*$^{+}$ and *Mx1Cre*$^{+}$ mice 6 weeks after transplantation. (h) Lineage donor (CD45.2) chimerism of competitive transplants 64 weeks after engraftment (40 weeks after secondary transplantation). (mean±SD, n=5; *p<0.05). (i) Confocal Q-FISH to measure the telomere length in *Rps14*$^{-/+}$*Mx1Cre*$^{+}$ and *Mx1Cre*$^{+}$ bone marrows 18 months after poly(I:C). (n=5 mice; n=12979 telomeres measured for *Mx1Cre*$^{+}$ and n=11935 telomeres measured for *Rps14*$^{-/+}$*Mx1Cre*$^{+}$*;* **p<0.001*).* Representative confocal images showing telomeres in nucleated, DAPI-positive cells.

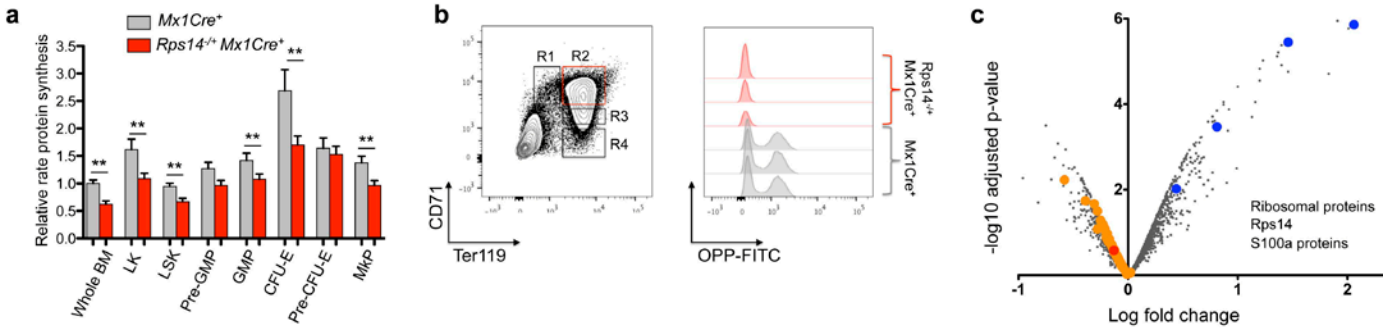

Supplementary figure 3

Supplementary figure 3: Reduced protein synthesis in *Rps14* haploinsufficient cells. (a) OP-Puro incorporation in bone marrow (BM) hematopoietic stem and progenitor cell populations in vivo 1 h after administration. Quantification of OP-Puro fluorescence reflecting protein synthesis rate in hematopoietic stem and progenitor cells relative to unfractionated bone marrow. Relative protein synthesis relative to unfractionated bone marrow (mean±SD, n=5; **p<0.001). (b) Representative flow blots showing the gating strategy for determination of OP-Puro incorporation in erythroid progenitor cell populations. (c) Volcano plot showing the log fold change of protein expression (X-Axis) to the –log10 adjusted p-value. Orange dots highlight all ribosome associated proteins, blue dots S100a proteins and the red dot Rps14.

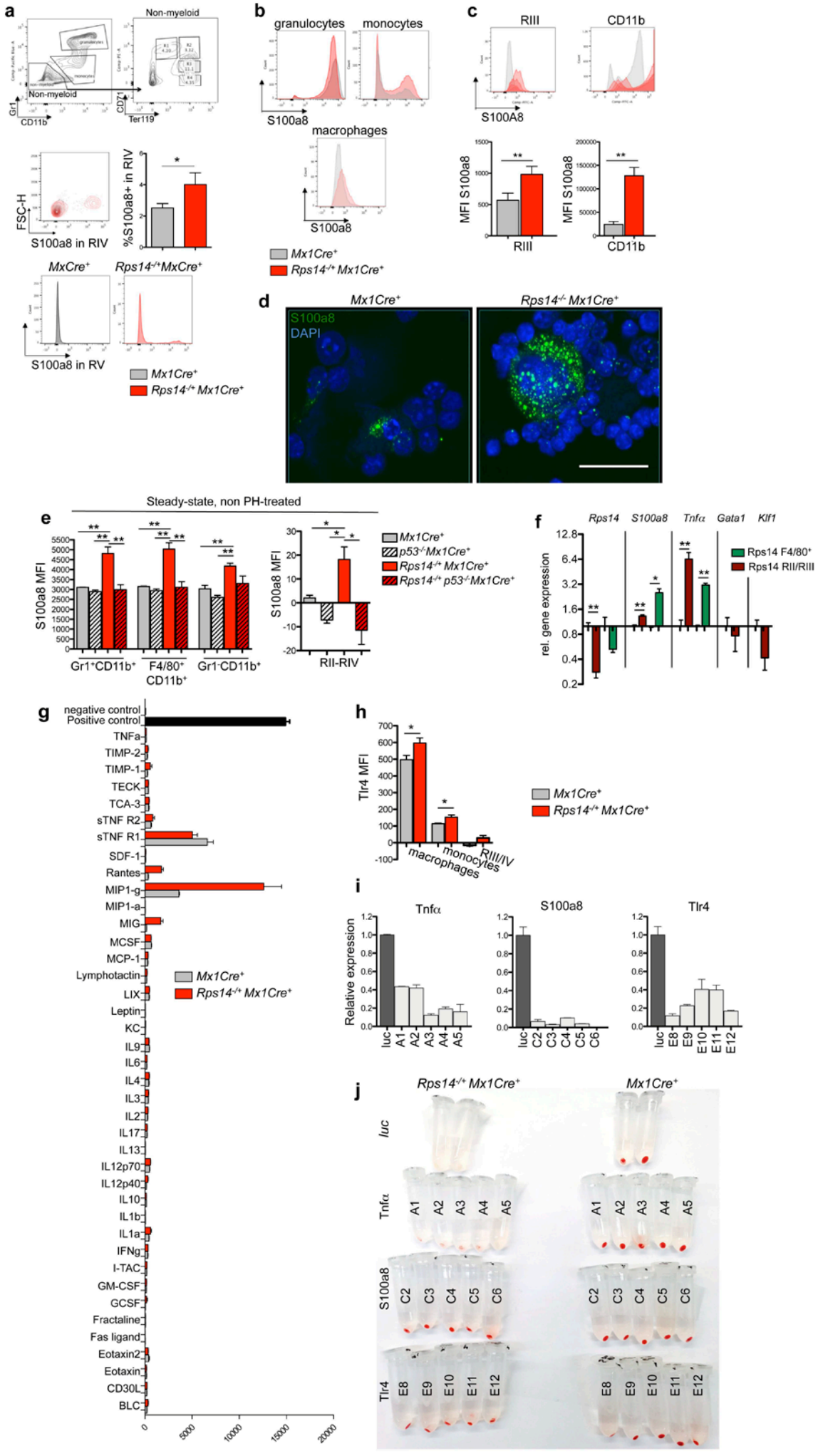

Supplementary information for figure 4

Supplementary figure 4: S100a8 is significantly up-regulated in *Rps14* haploinsufficient bone marrows, is regulated by *p53* induction, and is necessary for the erythroid differentiation defect. (a) Gating strategy for validating the up-regulation of S100a8 in erythroid progenitor populations (CD71/Ter119) and Gr1/CD11b-positive cells. Whole bone marrow was stained with Gr1, CD11b, Ter119 and CD71. Erythroid progenitors were gated from the non-myeloid cell population ($Gr1^{-}CD11b^{-}$). Representative flow blot showing S100a8 positive cells within the RIV population in $Rps14^{-/+}Mx1Cre^{+}$ and $Mx1Cre^{+}$mice (red: $Rps14^{-/+}Mx1Cre^{+}$ and grey). Quantification of the frequency of S100a8 expressing cells within the RIV population. (mean±SD, n=5; *p<0.05). Histogram showing S100A8 expression in the RIV population. (b) Histograms depicting S100a8 expression in granulocytes ($Gr1^{high}CD11b^{+}$), monocytes ($Gr1^{low}CD11b^{+}$) and macrophages ($CD11b^{+}F4/80^{+}$). (c) Histograms showing S100a8 expression in transplant experiments of 18 months old whole bone marrow cells in young recipients (compare Figure 2) 6 weeks after transplantation. Mean fluorescence intensity (MFI) of S100a8 in the RIII population and in monocytes in $Rps14^{-/+}Mx1Cre^{+}$ (n=5) and $Mx1Cre^{+}$ mice (n=4); (mean±SD; **p<0.001). (d) S100a8 (green) immunofluorescence on lineage-depleted whole bone marrows of $Rps14^{-/+}Mx1Cre^{+}$ (n=5) and $Mx1Cre^{+}$ mice (n=4). Nuclei are highlighted by DAPI staining. (e) Mean fluorescence intensity (MFI) of S100a8 expression in $Gr1^{+}CD11^{+}$ granulocytes, $Gr1^{-}CD11b^{+}$ monocytes, $F4/80^{+}$ macrophages and RII-RIV erythroblasts in $Mx1Cre^{+}$, $p53^{-/-}$, $Rps14^{-/+}Mx1Cre^{+}$ and $Rps14^{-/+}p53^{-/-}Mx1Cre^{+}$ mice 12 weeks after poly(I:C) (mean±SD, n=3; *p<0.05; *p*<0.001). (f) Quantification (qt-RT-PCR) of *Rps14*, *S100a8*, *Tnfα, Gata1* and *Klf1* expression in sort-purified RII/III erythroblasts (dark red) and $F4/80^{+}$ macrophages (green). The expression values are relative to $Mx1Cre^{+}$ control cells which were normalized to 1. (mean±SD, n=5; *p<0.05). (g) Intensity of expression of 40 cytokines detected by the cytokine expression array compared to negative and positive control. Fluorescence intensity normalized to background signals of inflammatory cytokines in bone marrows from $Mx1Cre^{+}$ and $Rps14^{-/+}Mx1Cre^{+}$ mice 12 weeks after the induction of the *Rps14* excision with poly(I:C). Log10 scale. (mean±SD, n=4). (h) Mean intensity fluorescence (MFI) of TLR4 on monocytes and macrophages [mean±SD, n=4 (MxCre), n=5 Rps14); *p<0.05)]. (i) Knockdown validation of shRNA targeting Tnfα, S100a8 and Tlr4 in ckit+ HSPC 6 days after transduction and selection with Puromycin compared to HSPC transduced with luc control shRNA. Efficient knockdown was confirmed for each of the 5 shRNA applied in the experiments. A1-5, C2-6 and E8-E12 highlights the different shRNA that were tested in the experiment (3 replicates per shRNA). (j) Cell pellets of $ckit^{+}$ HSPC derived from either $Mx1Cre^{+}$ and $Rps14^{-/+}Mx1Cre^{+}$ mice and transduced for 48 hours with shRNA and then subjected to erythroid differentiation in the presence of puromycin for additional 7 days *in vitro*. A1-5, C2-6 and E8-E12 highlights the different shRNA that were tested in the experiment (3 replicates per shRNA; representative pictures are shown).

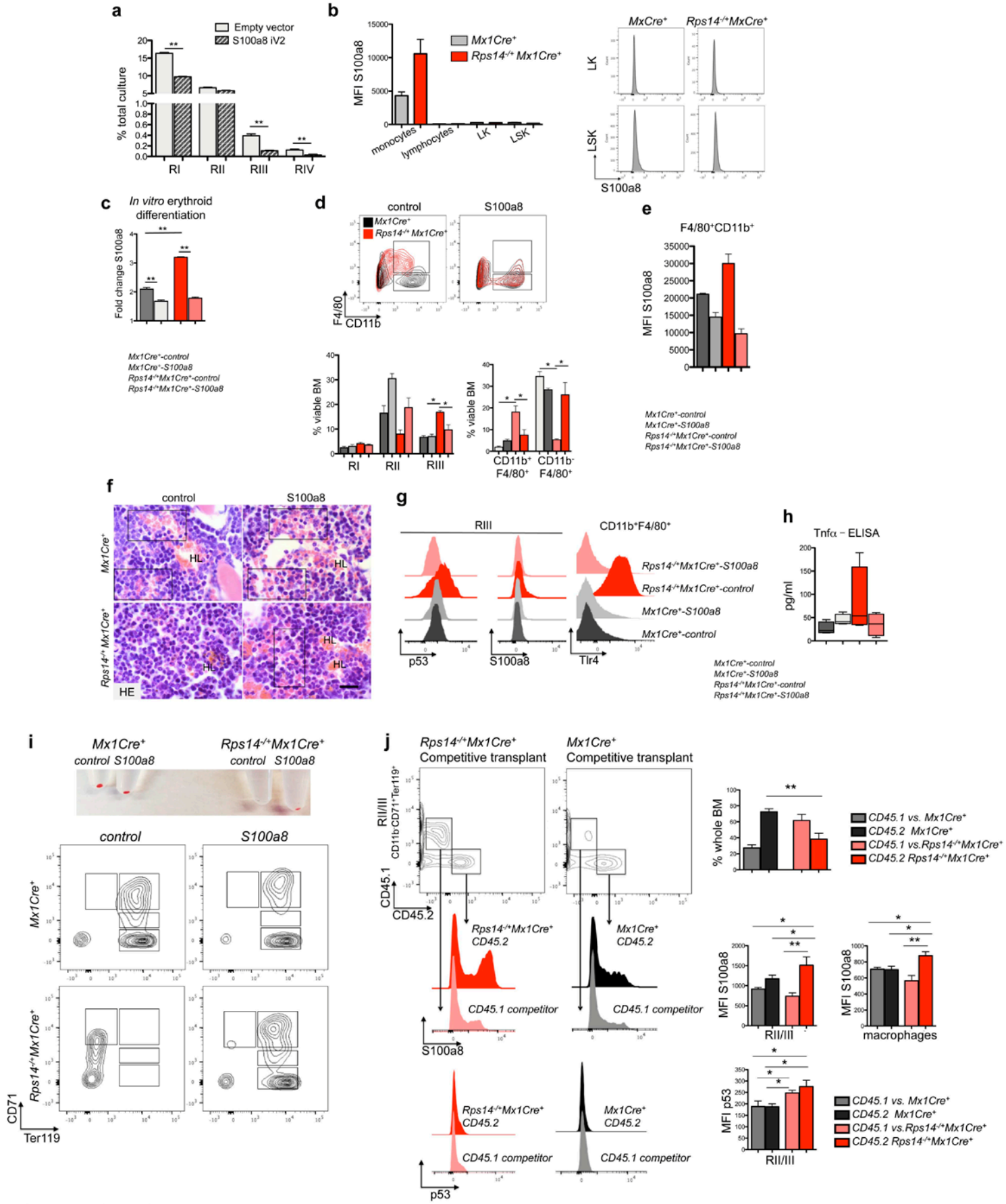

Supplementary figure 5

Supplementary figure 5: S100a8 is essential for the erythroid differentiation defect due to *Rps14* haploinsufficiency (a) ckit$^+$ wild-type HSPCs were transduced with S100a8 overexpression vectors or empty vector. 48 hours after transduction, GFP$^+$ cells were sort-purified and subsequently subjected to erythroid differentiation for 5 days. Frequency of RI-RIV erythroid progenitor populations in the culture after 5 days. (mean±SD; **p<0.001). (b) Mean fluorescence intensity (MFI) of S100a8 in the monocytes, lymphocytes, LK and LSK in *Rps14*$^{-/+}$*Mx1Cre*$^+$ (n=5) and *Mx1Cre*$^+$ mice (n=4). (c) Quantification of mean fluorescence intensity of S100a8 relative to the negative control (=1) Gr1^{low}CD11b$^+$ monocytes and (mean±SD, n=3 biological replicates; **p<0.001) confirming the downregulation of S100a8 after transduction with S100a8 sgRNA/Cas9 or NTG. (d) ckit+ HSPCs were transduced with a lentiviral vector expressing Cas9 and an sgRNA targeting S100a8 or control (non-targeting guide) and were transplanted 24 hours after infection into lethally irradiated wild-type recipients. 6 weeks after transplantation, recovered hematopoiesis in the transplanted mice was confirmed and PH was injected to induce hemolysis. 6 days after the first dose of PH, the bone marrow was harvested. Representative flow plots of the macrophage (CD11b$^+$F4/80$^+$) and monocyte (CD11b$^+$F4/80$^-$) population in *Rps14*$^{-/+}$*Mx1Cre*$^+$ (n=5) and *Mx1Cre*$^+$ mice (n=5) transduced with either control:Cas9 or S100a8 sgRNA:Cas9 6 days after induction of hemolysis with PH. Quantification of the erythroid progenitor populations (RI-III; RIV is shown in main figure 5) and macrophage and monocyte population. mean±SD, n=5; *p<0.05. (e) Quantification of the MFI of S100a8 expression in macrophages. (mean±SD, n=5). (f) HE-staining of bone marrows from *Rps14*$^{-/+}$*Mx1Cre*$^+$ or *Mx1Cre*$^+$ mice transduced with either control:Cas9 or S100a8 sgRNA:Cas9. HL=hemolysis; inserts show enucleated red blood cells. Scale bar: 50µm. (g) Histograms showing representative expression of p53 and S100a8 in RIII erythroblasts and Tlr4 expression in macrophages. (h) Tnfα was determined in enzyme linked immunosorbent assay (ELISA) in the bone marrow serum in in *Rps14*$^{-/+}$*Mx1Cre*$^+$ (n=5) and *Mx1Cre*$^+$ mice (n=5) transduced with either control:Cas9 or S100a8 sgRNA:Cas9, 6 days after induction of hemolysis with PH. (i) Lineage-negative cells from *Rps14*$^{-/+}$*Mx1Cre*$^+$ (n=3) and *Mx1Cre*$^+$ mice (n=3) were purified using bead-separation and transduced with control:Cas9 or S100a8 sgRNA:Cas9. After 48 hours, positively transduced, GFP$^+$CD71$^+$Ter119$^{low-intermediate}$ RI/RII erythroid progenitor cells were sort-purified and subjected to erythroid differentiation *in vitro* for another 48 hours. Representative cell pellets harvested after 48 hours are shown as well as representative flow plots of CD71/Ter119 staining. (j) Aged *Rps14* or *Mx1Cre*$^+$ control whole bone marrow cells (18 months) were mixed in a 1:1 competition and the expression of S100a8 and p53 was analyzed after 4 months when the mice presented with progressive anemia. S100a8 and p53 expression was analyzed by intracellular flow cytometry in competitor cells (CD45.1) and *Rps14* haploinsufficient or *Mx1Cre*$^+$ cells (CD45.2), respectively, in the RII/III population or macrophages. The gating on the CD45.1 and CD45.2 within the RII/III population is shown representatively and representative histograms analyzing S100a8 or p53 expression are presented. The mean fluorescence intensity of S100a8 and p53 within these populations and in the CD45.1/CD45.2 fraction within the F4/80$^+$ macrophage compartment was quantified. (mean±SD; *p<0.05; **p<0.001).

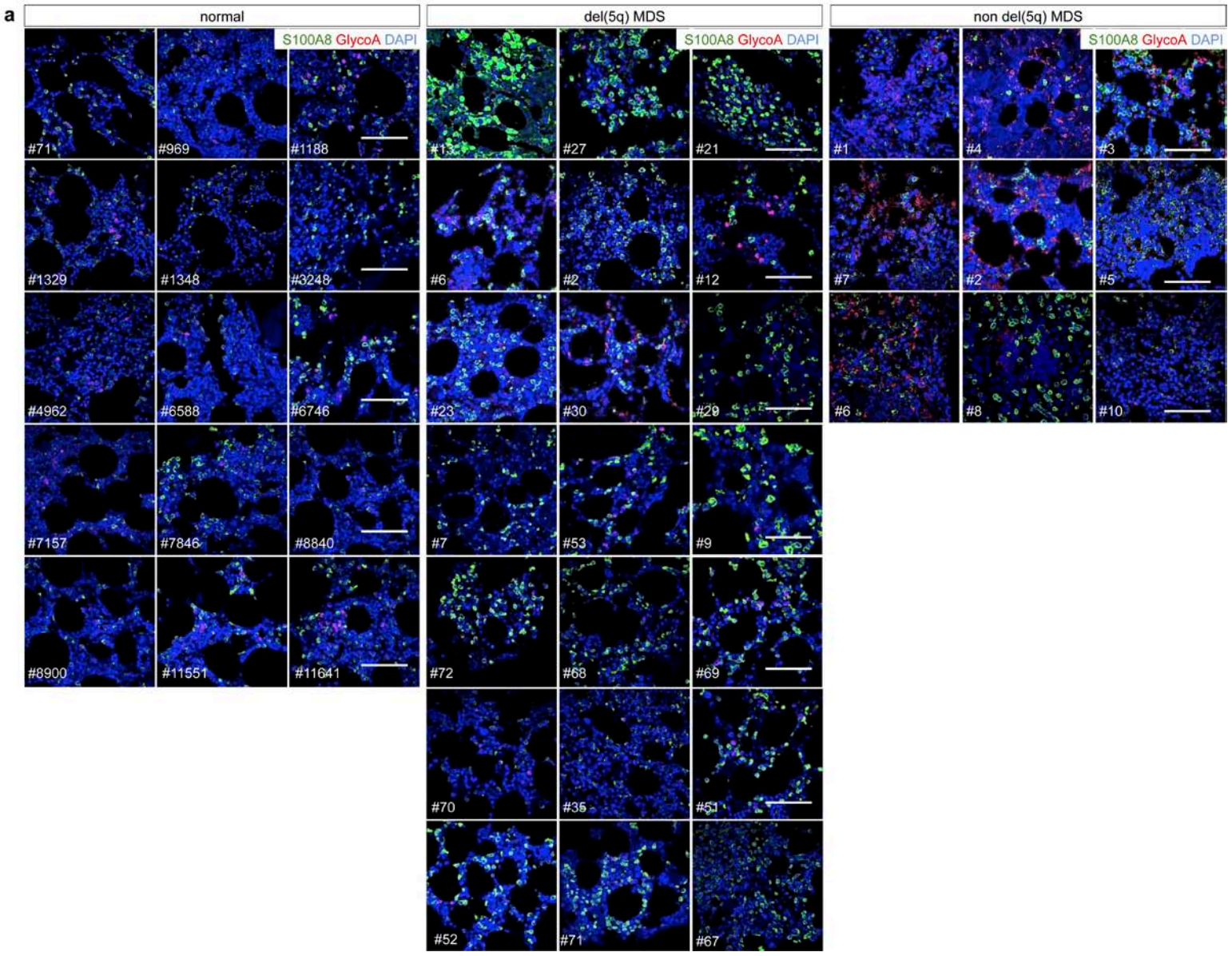

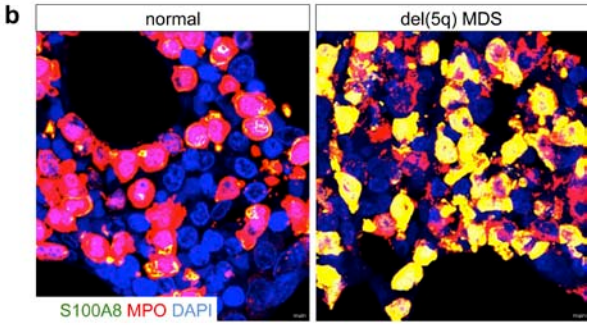

Supplementary figure 6

Supplementary figure 6: Images of co-immunoflurescent staining of Glycophorin A (GlyA), S100A8 and DAPI as a nuclear staining in normal bone marrows (n=15), del(5q) MDS (n=20) patients and normal karyotype MDS (non del(5q); n=9) and. DAPI (blue), S100A8 (green), GlyA (magenta). Scale bars: 100µm. (b) Representative images of co-immunofluorescent staining of myeloperoxidase as a marker for myeloid cells and S100A8 shows a strong co-expression in *Rps14* haploinsufficient cells.

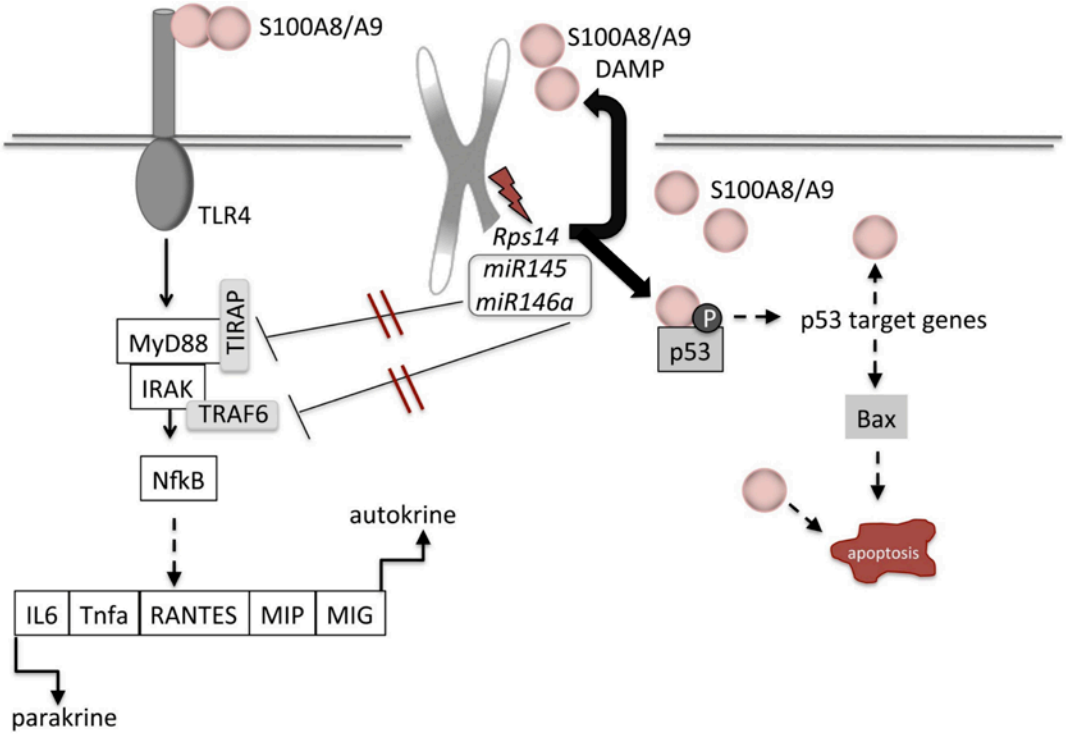

Supplementary figure 7

Supplementary figure 7: Collaborating effects of haploinsufficiency of genes on 5q. Deletion of the long arm of chromosome 5 leads to haploinsufficient expression of numerous genes. Based on our data we posit that the DAMP heterodimers S100A8/S100A9 are induced as a stress response upon ribosomal haploinsufficiency in monocytes, macrophages, and erythroblasts and contribute to the MDS phenotype. S100A8/A9 is an endogenous TLR4 ligand up-stream of TNFα leading to NF-kB activation and secretion of pro-inflammatory cytokines[1]. Our data demonstrate that S100a8 induced by Rps14 haploinsufficiency acts upstream of TLR4 in the erythroid differentiation defect. Of note, RPS14 and miR-145 are universally co-deleted in the 5q- syndrome and both converge on acting up- or downstream of TLR4 signaling[2-7], highlighting cooperating effects of genes on 5q. Our data further demonstrate that p53 is required for induction of S100a8 expression in *Rps14* haploinsufficient cells, and that recombinant S100a8 is sufficient to induce p53 activity in differentiating erythroid progenitor cells leading to a block in terminal erythroid differentiation. It was shown in recent reports that S100 proteins can be intracellularly located and regulate cell growth, cell-cycle progression and apoptosis by interacting with the relevant intracellular signal-regulation pathways. S100 proteins can interact with p53 and affect p53 transcriptional activity, resulting in expression changes of p53 target genes[1].

Gene symbol	Protein name	logFC	adj. p-value
S100a8	Protein S100-A8	2.057	0.0019735
Pglyrp1	Peptidoglycan recognition protein 1	2.013	0.00197349
Retnlg	Myeloid cysteine-rich protein	1.905	0.00197349
Mgp	Matrix Gla protein	1.826	0.005770276
S100a9	Protein S100-A9	1.4595	0.002959553
Ltf	Lactotransferrin	1.4575	0.005587191
Lcn2	Neutrophil gelatinase-associated lipocalin	1.4005	0.002959553
Chi3l1	Chitinase-3-like protein 1	1.397	0.004868785
Camp	Cathelin-related antimicrobial peptide	1.3705	0.003652307
Ngp	OS=Mus musculus GN=Ngp E=2 SV=1	1.3565	0.003848308
Apobr	Apolipoprotein B receptor	1.2345	0.004214127
Lrg1	Leucine-rich HEV glycoprotein	1.201	0.007654588
Padi4	Protein-arginine deiminase type-4	1.198	0.005221609
Hp	Haptoglobin	1.1555	0.01958689
Lyz2	Lysozyme C-2	1.1315	0.033817984
Anxa1	Annexin A1	0.997	0.009836916
Ear2	Eosinophil cationic protein 2	0.9915	0.170633883
Gys1	Glycogen [starch] synthase, muscle	0.924	0.025785806
Mmp9	Matrix metalloproteinase-9	0.907	0.05404763
Gda	Guanine deaminase	0.8985	0.025569514
Nfrkb	Nuclear factor related to kappa-B-binding protein	0.8675	0.01958689
Aldh3b1	Aldehyde dehydrogenase family 3 member B1	0.865	0.021200077
S100a11	Protein S100-A11	0.8115	0.04566109
Itgb2	Integrin beta-2	0.7905	0.037963425
Itgam	Integrin alpha-M	0.8055	0.026112389
Ncf2	Neutrophil cytosol factor 2	0.771	0.037963425

Supplementary Table 1: Differentially expressed proteins identified by iTRAQ-based mass spectrometry (adjusted p-value of <0.05)

			blasts		hemoglobin		ANC		platelets		ferritin	
Pat. Nr	IPSS-Score	WHO	frequency									
5q-2	intermediate-1	MDS, isolated 5q	0	%	9	g/dl	7936	/µl	634	/nl (GPT/l)	1938	ng/ml
5q-6	low risk	RCMD, 5q-	0	%	9	g/dl	n.a.	/µl	423	/nl (GPT/l)	954.3	ng/ml
5q-12	low risk	MDS, isolated 5q	0	%	6.279	g/dl	1290	/µl	146	/nl (GPT/l)	1324.2	ng/ml
5q-13	low risk	MDS, isolated 5q	0	%	8.694	g/dl	5860	/µl	136	/nl (GPT/l)	1238.2	ng/ml
5q-21	low risk	MDS, isolated 5q	0	%	10.626	g/dl	5930	/µl	546	/nl (GPT/l)	2424.8	ng/ml
5q-23	low risk	RA, 5q-	0	%	8.3	g/dl	4950	/µl	218	/nl (GPT/l)	8867	ng/ml
5q-27	intermediate-1	MDS, isolated 5q	0	%	10.143	g/dl	1480	/µl	102	/nl (GPT/l)	1745.1	ng/ml
5q-29	intermediate-1	MDS, isolated 5q	0	%	7.728	g/dl	1350	/µl	69	/nl (GPT/l)	6471.4	ng/ml
5q-30	low risk	RA, 5q-	0	%	10.5	g/dl	7700	/µl	674	/nl (GPT/l)	691.9	ng/ml
5q-35	low risk	MDS, isolated 5q	1	%	8.7	g/dl	1630	/µl	429	/nl (GPT/l)	454.4	ng/ml
5q-51	intermediate-1	MDS, isolated 5q	<1	%	8.7	g/dl	1240	/µl	70	/nl (GPT/l)	515.3	ng/ml
5q-52	n.d.	RCMD	3	%	10.3	g/dl	1600	/µl	287	/nl (GPT/l)	1880.2	ng/ml
5q-53	intermediate-1	RCMD, isolated 5q	4	%	8.4	g/dl	1000	/µl	467	/nl (GPT/l)	274.8	ng/ml
5q-68	n.d.	MDS, isolated 5q	<5	%	11.3	g/dl	2360	/µl	579	/nl (GPT/l)	383.7	ng/ml
5q-69	low risk	MDS, isolated 5q	1	%	8.2	g/dl	1870	/µl	384	/nl (GPT/l)	168	ng/ml
5q-70	low risk	MDS, isolated 5q	3.5	%	8.9	g/dl	2420	/µl	199	/nl (GPT/l)	n.d.	
5q-71	low risk	RAEB I, isolated 5q	2	%	8.4	g/dl	980	/µl	360	/nl (GPT/l)	275.5	ng/ml
5q-7	low risk	MDS, isolated 5q	0	%	8.6	g/dl	1240	/µl	280	/nl (GPT/l)	5880	ng/ml
5q-9	intermediate-1	MDS, isolated 5q	n.d.		6.7	g/dl	1782	/µl	160	/nl (GPT/l)	1758	ng/ml
5q-67	low risk	RCMD; 5q-	0	%	11.1	g/dl	11200	/µl	640	/nl (GPT/l)	316.5	ng/ml
5q-72	low risk	RCMD; 5q-	n.d.		n.d.		n.d.		n.d.		n.d.	
Non5q-1	intermediate-1	RAEB I	0	%	8.3	g/dl	2100	/µl	117	/nl (GPT/l)	427.9	ng/ml
Non5q-2	low risk	RCMD	0	%	13.8	g/dl	140	/µl	198	/nl (GPT/l)	148.1	ng/ml
Non5q-3	intermediate-1	RARS	0	%	8.8	g/dl	2390	/µl	42	/nl (GPT/l)	2743.0	ng/ml
Non5q-4	intermediate-2	RAEB II	0	%	8.1	g/dl	730	/µl	160	/nl (GPT/l)	2645.0	ng/ml
Non5q-5	low risk	RCMD	0	%	11.6	g/dl	5400	/µl	31	/nl (GPT/l)	n.a.	ng/ml
Non5q-6	intermediate-1	RCMD	0	%	6.9	g/dl	900	/µl	28	/nl (GPT/l)	533.2	ng/ml
Non5q-7	low risk	RCMD	0	%	11.2	g/dl	3900	/µl	282	/nl (GPT/l)	182.0	ng/ml
Non5q-8	intermediate-2	RAEB I	0	%	6.8	g/dl	770	/µl	95	/nl (GPT/l)	379.3	ng/ml
Non5q-9	n.a.	RCMD	0	%	10	g/dl	n.a.	/µl	172	/nl (GPT/l)	n.a.	
Non5q-10	intermediate-1	NA	0	%	8.7	g/dl	2600	/µl	329	/nl (GPT/l)	845.5	ng/ml
normal-7157	n.a.	n.a.	0	%	15.3	g/dl	5100	/µl	227	/nl (GPT/l)	n.d.	
normal -3248	n.a.	n.a.	0	%	12.1	g/dl	2700	/µl	249	/nl (GPT/l)	n.d.	
normal - 71	n.a.	n.a.		%	15.1	g/dl	2400	/µl	184	/nl (GPT/l)	n.d.	
normal- 1348	n.a.	n.a.	0	%	15.3	g/dl	3400	/µl	210	/nl (GPT/l)	n.d.	
normal -8840	n.a.	n.a.	0	%	16.2	g/dl	6500	/µl	190	/nl (GPT/l)	n.d.	
normal - 6588	n.a.	n.a.	0	%	15.2	g/dl	3800	/µl	200	/nl (GPT/l)	n.d.	
normal - 1329	n.a.	n.a.	0	%	13.1	g/dl	3600	/µl	180	/nl (GPT/l)	n.d.	
normal- 11551	n.a.	n.a.	0	%	13.9	g/dl	4000	/µl	212	/nl (GPT/l)	n.d.	
normal -11641	n.a.	n.a.	0	%	13.5	g/dl	3100	/µl	247	/nl (GPT/l)	n.d.	

			blasts		hemoglobin		ANC		platelets		ferritin	
Pat. Nr	IPSS-Score	WHO	frequency									
normal - 969	n.a.	n.a.	0	%	15.2	g/dl	4900	/µl	244	/nl (GPT/l)	n.d.	
normal -6746	n.a.	n.a.	0	%	16.6	g/dl	4600	/µl	166	/nl (GPT/l)	n.d.	
normal -4962	n.a.	n.a.	0	%	13.3	g/dl	2300	/µl	140	/nl (GPT/l)	n.d.	
normal -1188	n.a.	n.a.	0	%	13.6	g/dl	3100	/µl	205	/nl (GPT/l)	n.d.	
normal -8900	n.a.	n.a.	0	%	14.1	g/dl	4400	/µl	167	/nl (GPT/l)	n.d.	
normal -7846	n.a.	n.a.	0	%	12.5	g/dl	4000	/µl	247	/nl (GPT/l)	n.d.	

Supplementary table 2: Clinical data for bone marrow biopsies included in the study.

iTRAQ labeling			
114	115	116	117
RII/III Rps14 Heterozygote (n=4)	RII/III Wild Type Heterozygote (n=4)	RII/III Rps14 Heterozygote (n=4)	RII/III Wild Type Heterozygote (n=4)
process replicate 1		**process replicate 2**	

Supplementary Table 3: Samples included in the proteomic analysis

1 Ehrchen, J. M., Sunderkotter, C., Foell, D., Vogl, T. & Roth, J. The endogenous Toll-like receptor 4 agonist S100A8/S100A9 (calprotectin) as innate amplifier of infection, autoimmunity, and cancer. *Journal of leukocyte biology* **86**, 557-566, doi:10.1189/jlb.1008647 (2009).

2 Chang, K. H. *et al.* p62 is required for stem cell/progenitor retention through inhibition of IKK/NF-kappaB/Ccl4 signaling at the bone marrow macrophage-osteoblast niche. *Cell reports* **9**, 2084-2097, doi:10.1016/j.celrep.2014.11.031 (2014).

3 Starczynowski, D. T. & Karsan, A. Deregulation of innate immune signaling in myelodysplastic syndromes is associated with deletion of chromosome arm 5q. *Cell Cycle* **9**, 855-856 (2010).

4 Starczynowski, D. T. *et al.* Identification of miR-145 and miR-146a as mediators of the 5q- syndrome phenotype. *Nature medicine* **16**, 49-58, doi:10.1038/nm.2054 (2010).

5 Starczynowski, D. T. *et al.* TRAF6 is an amplified oncogene bridging the RAS and NF-kappaB pathways in human lung cancer. *The Journal of clinical investigation* **121**, 4095-4105, doi:10.1172/JCI58818 (2011).

6 Reynaud, D. *et al.* IL-6 controls leukemic multipotent progenitor cell fate and contributes to chronic myelogenous leukemia development. *Cancer Cell* **20**, 661-673, doi:10.1016/j.ccr.2011.10.012 (2011).

7 Rhyasen, G. W. *et al.* Targeting IRAK1 as a therapeutic approach for myelodysplastic syndrome. *Cancer Cell* **24**, 90-104, doi:10.1016/j.ccr.2013.05.006 (2013).